FINITE ELEMENT MODEL UPDATING OF THE WELDED JOINTS IN A TUBULAR H-FRAME

B. Horton [a,b], H. Gurgenci[a,b], M. Veidt[a], M.I. Friswell[c]

[a] The University of Queensland, Department of Mechanical Engineering

[b] Co-operative Research Centre for Mining Technology and Equipment (CMTE), Australia

[c] The University of Wales Swansea, Department of Mechanical Engineering

ABSTRACT

Representation of individual welded joints within large fabricated structures has always been problematic, especially when the aim is to predict dynamic structural behaviour. In this paper, the Finite Element model updating of a welded tubular H-frame is attempted using an iterative eigenvalue sensitivity approach. Two methods for parameterising the welded connections of the H-frame are investigated - a simple spring connectivity method and a geometric offset approach. Using experimental modal data, the updating of the H-frame FE model is attempted and the results from the different joint representation schemes presented.

NOMENCLATURE

M, K	mass, stiffness matrix
λ_i	i^{th} system eigenvalue
ω_i	i^{th} undamped natural frequency
ζ_i	i^{th} damping ratio
ϕ_i	i^{th} mass normalised mode shape vector
θ, θ_i	design parameter vector, i^{th} design parameter
z, z_i	analytical modal quantity vector, i^{th} analytical modal quantity
z_m	measured modal quantity vector
S	modal sensitivity matrix
θ^j	value at the jth iteration step
$\bar{\omega}$	normalised frequency error ($\frac{\Delta\omega}{\omega_{mi}} = \frac{\omega_i - \omega_{mi}}{\omega_{mi}}$)
D	$S_o^T W_{\varepsilon\varepsilon} S_o + \alpha W_{\theta\theta}$
E, I, A, ρ	Young's modulus, 2nd moment of area, cross sectional area, density

1 INTRODUCTION

The way that a welded connection is represented by a Finite Element Model(FEM) is determined mainly by the type of application needed by the analyst. If the localised stress field of the welded connection is of primary concern, a detailed 3D brick or plate model consisting of thousands of degrees of freedom would be an appropriate choice. Often however the main interest in FE modelling is the global representation of a structure which contains dozens of welded joints. Under these circumstances it is computationally prohibitive and often unnecessary to extend the same level of modelling detail to the entire structure. For example, structures such as the boom of a crane consist mostly of beam type members and can be modelled quite effectively using beam elements. The problem then arises as to how the welded joints connecting these beam members should be modelled.

Recently several authors have investigated the influence of welded joints on the FE modelling of beam type structures. The work of Lindholm [1], Alvin [2] and Mottershead et al. [3] have all shown that for even simple welded structures the modal properties estimated by an FE model can differ considerably to those obtained experimentally. A common conclusion was that the source of the modelling errors was due largely to the inadequate representation of the welded joints.

The work reported here is part of a larger CMTE project that is aiming to characterise mechanical structures, such as a dragline boom, by using environmental excitations. Early in this project it became apparent that the principal obstacle to dynamic characterisation of large welded structures was the lack of knowledge of individual welded joints. This paper reports the investigation of welded joints in a simple H-frame and compares two approaches for joint parameterisation. For each joint modelling approach the terms parameterising the joint are refined by updating the H-frame FE model. The FEM updating method adopted was an iterative modal sensitivity approach.

2 FE UPDATING USING AN ITERATIVE EIGENVALUE SENSITIVITY APPROACH

A frequently used method for updating FE models are the sensitivity based methods which utilize modal parameter sensitivities(eigenvalues, eigenvectors) . A recent review of these methods is provided by Friswell and Mottershead [4]. The underlying approach of the Forward Modal Sensitivity (FMS) methods is the expansion of the modal data set z, as a 1st order Taylor series about a set of specified design parameters θ. For the updating exercises considered in this paper the approach advocated by Mottershead et al. [3] will be followed. Only Eigenvalue measurements will be used in updating, while the measured mode shape data will only

be used to pair off modes generated by an *FE* model. The contents of the modal output vector z can then be chosen to contain only the normal mode frequencies, for example $z_1 = \lambda_1 \equiv \omega_1^2$. The fundamental equation for the forward sensitivity methods is given by (1), where $\varepsilon(\equiv z_m - z(\theta))$ is a vector of modal residuals. The dimensions of the relevant terms in (1) are $\delta z \in R^n$, $\delta\theta \in R^d$ and $S^j \in R^{n \times d}$, where n and d represent the number of measured modes and the number of design parameters, respectively.

$$\varepsilon = \delta z - S^j \ \delta\theta \quad (1) \qquad \frac{\partial \lambda_j}{\partial \theta_r} = \phi_j^T \left[\frac{\partial K}{\partial \theta_r} - \lambda_j \frac{\partial M}{\partial \theta_r} \right] \phi_j \quad (2)$$

If z^j represents the current model prediction state and z_m represents the measured state, the perturbation vector δz is expressed as $\delta z = z_m - z^j$. Similarly the design variable perturbation vector $\delta\theta$ takes the form $\delta\theta = \theta^{j+1} - \theta^j$. When (1) is solved for $\delta\theta$, the new (or updated) design state θ^{j+1} is then calculated. The elements of the sensitivity matrix S^j represent the sensitivities of the eigenvalues to each design parameter θ. These can be calculated by a method proposed by Fox and Kapoor et al. [5], where the eigenvalue λ sensitivity for the system $K\phi = \lambda M\phi$ is presented by equation (2) - note $\phi_i^T M \phi_j = \delta_{ij}$. Because equation (1) formulates a linear problem by truncating the higher order terms in the Taylor series, it becomes necessary to solve (1) through Gauss-Newton iteration. At each iteration step the modal residual ε is minimized in a least squares sense, by minimizing an appropriate cost function J.

$$J = \varepsilon^T \ W_{\varepsilon\varepsilon} \ \varepsilon + \alpha\delta\theta^T \ W_{\theta\theta} \ \delta\theta \quad (3)$$

$$\delta\theta = [S^T \ W_{\varepsilon\varepsilon} \ S + \alpha W_{\theta\theta}]^{-1} S^T \ W_{\varepsilon\varepsilon}\delta z \quad (4)$$

A commonly used cost function and the associated update equation is presented by equations (3)-(4)(see for example Link [6], Collins et al. [7]). A brief derivation linking the residual equation (1) to the update equation (4) is provided in the Appendix. The weighting matrices $W_{\varepsilon\varepsilon}$ and $W_{\theta\theta}$ are used to indicate the confidence that the analyst has in the measurements ε and design parameters θ respectively. In this paper the measurement residual matrix was assigned to unity (ie: $W_{\varepsilon\varepsilon} = I$), while the design parameter matrix $W_{\theta\theta}$ was defined as a diagonal matrix, with the diagonal terms equal to the reciprocal of the component variances. The variance for each design parameter was chosen to be a fixed percentage of the current design parameter value. The inclusion of the α in (3) allows the design parameter term to be weighted relative to the residual term. For an overdetermined system of equations (more measurements than design parameters) the scalar α controls the speed of convergence of the update - see for example Blakely and Walton [8]. A large value for α causes slower convergence than a smaller α. In all updating exercises a consistent (or overdetermined) problem has been formulated, ie: only cases with more measurements than design parameters have been considered.

3 A REVIEW OF CURRENT WELDED JOINT MODELLING

In the proceeding sections a review of two methods for representing the compliance of welded connections within Finite Element models will be discussed. Although the presented

methods can easily be extended for the case of a three dimensional joint, the simpler case of representing a joint in two dimensions will be discussed here.

3.1 The Spring Joint Model

The spring joint *FE* model is shown by Figure 1. One of the key features of the spring model is that the two members being joined are physically separated by a massless rigid element (or stiff beam). When beam elements are being used, the inclusion of the rigid element conserves the mass of the structure. The rigid element represents the length from the beam neutral axis to the connection point. The connection of the two members is then achieved via a series of translational (k_X, k_Z) and rotational $(k_{\theta Y})$ springs which connect a pair of coincident nodes. In the updating exercises presented in this paper, the rigid connection was represented by a massless beam element with an increased Young's modulus $(E_{stiff} = 5 \times E)$.
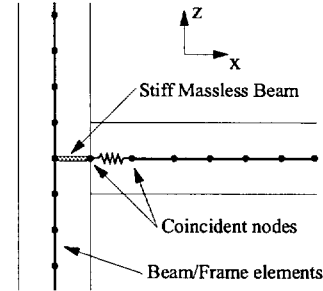

Figure 1: Spring joint model

3.2 The Geometric Offset Joint Model

The geometric offset approach to joint modelling was first developed by Mottershead et al. [3], and later reformulated by Ahmadian et al. [9] in the form of the *partly rigid* beam element. Ahmadian's formulation of the partly rigid beam element stems from the assumption that the stiffness of the joint is greater than the surrounding regions. This stiff joint region may then be regarded as being partly rigid. To represent this stiff region, Ahmadian defined the *partly rigid* beam element shown in Figure 2. If k_e represents the standard stiffness ma-
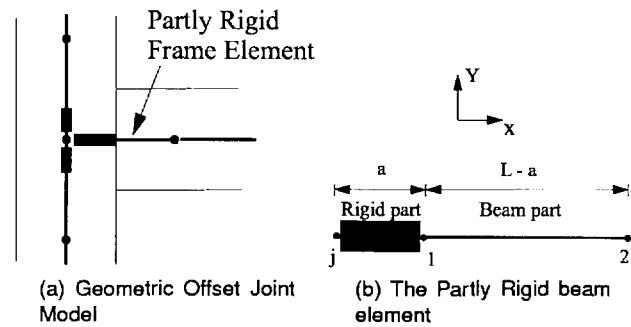

(a) Geometric Offset Joint Model

(b) The Partly Rigid beam element

Figure 2: Geometric Offset Joint Modelling

trix for an Euler-Bernoulli beam element of length (L-a), and $d_{12} = \{y_1 \ \theta_1 \ y_2 \ \theta_2\}$ represents the dof vector for the beam element, Ahmadian et al. [9] derived the stiffness matrix for the

partly rigid beam element via the co-ordinate transformation $d_{j2} = \{(y_1 - a\theta_1)\,\theta_1\, y_2\, \theta_2\} = Qd_{12}$. The reverse co-ordinate transformation $d_{12} = Td_{j2}$ then allows the stiffness matrix for the partly rigid element to be defined by $k_{er} = T^T k_e T$ as shown by equation (5). Similarly, the rigid offset can also be incorporated into the axial stiffness component giving a frame element with an $AE/(L - a)$ axial stiffness co-efficient. In the updating exercises presented in this paper, a fixed offset a_0 was applied to the element mass matrix ie: $m_{er} = f(L, a_0)$, while a variable offset a was applied to the elemental stiffness matrix ie: $k_{er} = f(L, a)$. In other words, only the stiffness matrix is updated while the mass matrix remains untouched through the updating process.

$$
k_{er} = EI \begin{bmatrix}
\frac{12}{(-a+L)^3} & \frac{-6(L+a)}{(a-L)^3} & \frac{12}{(a-L)^3} & \frac{6}{(a-L)^2} \\
\frac{-6(L+a)}{(a-L)^3} & \frac{-4(a^2+aL+L^2)}{(a-L)^3} & \frac{6(a+L)}{(a-L)^3} & \frac{2(2a+L)}{(a-L)^2} \\
\frac{12}{(a-L)^3} & \frac{6(a+L)}{(a-L)^3} & \frac{12}{(-a+L)^3} & \frac{-6}{(a-L)^2} \\
\frac{6}{(a-L)^2} & \frac{2(2a+L)}{(a-L)^2} & \frac{-6}{(a-L)^2} & \frac{4}{-a+L}
\end{bmatrix}
\tag{5}
$$

4 DESCRIPTION OF H-FRAME TEST ARTICLE

The H-frame test article considered for the model updating exercise is presented in Figure 3. The H-frame consists of three Rectangular Hollow Sections (RHS) joined at right angles via fillet and butt bevel welds. The cross section used for all RHS members was $40 \times 40 \times 2.5 mm^3$. Figure 3 also shows the global co-ordinate system used to describe the deformations of the H-frame. To generate the experimental Frequency Re-
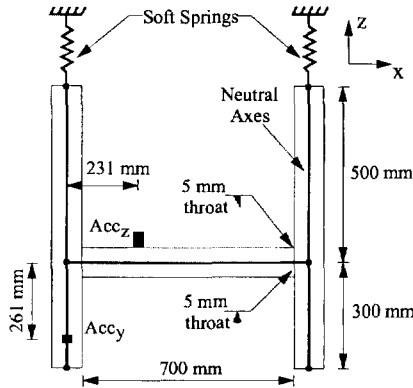

Figure 3: H-frame test article

sponse Functions (FRF) needed for determining the modal properties of the H-frame, a series of impact excitation tests was conducted. To remove the influence of boundary conditions from the tests, the H-frame was tested in a FREE-FREE configuration. This was accomplished by suspending the H-frame via two elastic straps (or soft springs) as shown by Figure 3. The impact tests involved varying the point of hammer excitation while measuring the vibration response at a single fixed accelerometer point. The accelerometer configuration used during the impact tests is shown in Figure 3. Note that although two accelerometers are shown (Acc_Z and Acc_Y) only responses from the Z direction accelerometer (ie, Acc_Z) were measured. The excitation of the H-frame was also limited to the ZX plane, ie: only impacts in the Z and X directions were applied.

The acquisition of the excitation and response data, was obtained using an Iotech Wavebook data acquisition system. A sampling frequency of 20000 [Hz] was used in conjunction with an anti aliasing filter with a cutoff frequency of 1102 [Hz]. In generating the experimental FRFs a baseband spectral analysis was performed (ie: zoom frequency analysis was NOT attempted). A block size of $N = 2^{16}$ was used giving a frequency resolution of 0.305 [Hz]. To combat the spectral leakage problem associated with processing truncated time domain data, a 2 % exponential window was used to weight all response measurements and a transient window placed over all excitation time histories. A total of 28 Receptance FRFs were generated from the H-frame impact tests.

4.1 Extraction of Modal properties from Experimental FRFs

From the experimentally generated Receptance FRFs the H-frame's modal properties were extracted by applying a two stage System Identification (SI) process. The objective of the SI process was to identify the poles ($\lambda_r \equiv -\zeta_r\omega_r + j\omega_r\sqrt{1 - \zeta_r^2}$) and residues R_r of equation (6) - the parametric FRF equation for a viscously damped system.

$$
H(\omega)_{jk} = \sum_{r=1}^{N} \frac{R_r}{s - \lambda_r} + \frac{R_r^*}{s - \lambda_r^*}
\tag{6}
$$

The first stage of the identification process consisted of generating pole estimates from local FRF curve fits. The algorithm used to do this was the time domain Complex Exponential Method (CE), see for example Brown et al. [10]. The problem with the using the CE method is that the order of the system being curve fitted has to be severely overestimated in order to get accurate FRF curve fits. The overestimation in the number of poles in a given FRF results in spurious computational modes also being generated. The difficulty then arises of having to separate the true system poles from the computational poles. To identify the true system poles, the frequency domain curve fitting algorithm proposed by Levy [11] and implemented by MATLAB© [12], was used in parallel with the CE method. By running the two methods in parallel the true poles were identified as those being in common to both methods. The validity of the common poles was also verified by visual inspection of the FRF plots.

After using the two local curve fits to generate estimates of the H-frame's dynamic poles, the second stage of the system identification process was to refine the pole estimates by performing a global curve fit using all 28 of the experimental FRFs. The global curve fit method used was a frequency domain method derived by Balmes [13] and implemented by the Structural Dynamics Toolbox (Balmes [13]). A summary of the identified experimental poles is presented in Table 1

5 FINITE ELEMENT MODELLING OF THE H-FRAME

The Structural Dynamics Toolbox developed by Balmes [13], was used to generate a Finite Element (FE) model of the H-frame. Twelve dof Euler-Bernoulli beam elements were used. However to limit the FE analysis to a single plane, the active degrees of freedom for the FE models were reduced to X and

	Measured modes							
	1	2	3	4	5	6	7	8
ω_i [Hz]	77.13	137.60	300.90	404.98	482.23	911.64	960.79	979.89
ζ_i [-]	0.0049	0.0022	0.0009	0.0007	0.0007	0.0011	0.0008	0.0010

TABLE 1: Experimental undamped natural frequencies and damping ratios

Mesh case ⇓	FE modes							
	1	2	3	4	5	6	7	8
Natural frequencies normalised with Mesh A								
Mesh A	1	1	1	1	1	1	1	1
Mesh B	1	1	1	1	0.999	0.999	0.998	0.994
Mesh C	1	1	1	1	0.999	0.999	0.998	0.994
Mesh D	1	1	1	1	0.999	0.999	0.998	0.994
Mesh C_a	0.995	0.993	0.976	0.977	0.979	0.998	0.988	0.976

TABLE 2: FEM mesh comparison for the prototype model

Z translations and Y rotations, ie all elements used were reduced to the Euler-Bernoulli frame element. Before including the effects of the welded joints into the FE models, a prototype model was developed to investigate the effect of the element mesh density on the convergence of the predicted natural frequencies. The prototype model consisted of meshing the neutral axes (see Figure 3) of the H-frame members with frame elements. In the prototype models no attempt was made to represent the welded joints. Element connections at the joints were assembled in an identical manner to the surrounding elements. Four element mesh configurations for the prototype model were considered, cases A(4,2,4), B(8,4,8), C(16,8,16) and D(32,16,32) - where (i, j, k) represent the number of elements along the horizontal and lower and upper vertical segments respectively. The normalised natural frequencies predicted by the prototype FE models are summarised in Table 2 for the first 8 modes. The natural frequencies have been normalised with respect to mesh case A, where it can be seen that the first 8 modes have converged for mesh cases B, C and D. The influence of the mass loading effect caused by the two accelerometers can also be seen from the results for mesh case C_a - here the same mesh density as case C was used however point masses offset by massless rigid beams were also added.

Using the mesh case C_a prototype model, the experimental modes listed in Table 1 were paired off with the corresponding FE modes. Table 3 shows the MAC correlation values for the case were the measured modes are first expanded to full FE dof size using a SEREP (O'Callahan et al. [14]) expansion process. The MAC numbers presented in Table 3 show strong matches for all measured modes except the mode at 960.79 [Hz]. Given that the H-frame is really a 3 dimensional structure as compared to the 2-D FE model considered here, the unpaired mode is most likely an out of plane torsional mode.

6 RESULTS: UPDATING THE PROTOTYPE FE MODEL

Before including the representation of the welded joints into the prototype FE model, a useful exercise highlighting the localized nature of the FE modelling errors, can be achieved by updating the C_a prototype model. Consider first the updating exercise where the flexural rigidity (EI) for all 64 frame elements are updated in a global sense, ie: a single design parameter common to all elements was chosen. When the first 5 measured modes are used to drive the global update, the converged updated model, see Table 4(a), shows little improvement over the original model. Rather than uniformly forcing the normalised frequency errors $\bar{\omega}$ to zero, modes 2 and 5 are improved at the expense of increasing the errors for the remaining three modes. The failure of this global update however, was not entirely unexpected. If a linear global parameter such as E or ρ was truly responsible for the modelling errors, this should have been observed via a more even distribution in the original frequency errors - for example doubling E should increase the FE modes by a factor of $\sqrt{2}$. Looking at the initial FE frequency errors in Table 4(a), it can be seen that the errors are not proportionally constant between the modes. This fact provides a strong indication that the true source of modelling error is localised at the welded connections. It can further be argued that certain modes will tend to deform the region surrounding the joint more so than others. A consequence then, is that modes which cause significant deformations of the joint, for example modes 2 and 5, can then be expected to have the largest differences between their corresponding measured modes.

To further emphasize this point consider the case of only locally updating the elements within the immediate vicinity of the welded connection, ie: each welded T-joint is modelled by 3 frame elements. Let the flexural rigidity (EI_x) for the 2 horizontal elements be one design parameter and the flexural rigidity of the remaining 4 vertical elements (EI_z) be a second. Using the first 5 measured modes to again drive the local update, Table 4(b) summarises the normalised natural frequency errors $\bar{\omega}$ and the design parameter perturbations. The results in Table 4(b) show that the modes for the updated FE model have significantly improved.

Exper	Analytical Modes [Hz] ⇒							
Modes [Hz]	1	2	3	4	5	6	7	8
⇓	78.51	147.31	298.90	408.03	523.31	957.34	1013.35	1310.70
	Expanded modes: SEREP expansion							
77.13	**97.39**	0.19	0.00	0.04	4.30	13.77	0.40	0.16
137.60	0.61	**93.09**	1.33	0.00	0.09	2.45	11.69	5.28
300.90	0.21	0.12	**75.39**	7.37	0.21	13.36	0.30	1.36
404.98	0.54	4.71	1.94	**85.21**	0.18	2.83	3.07	1.80
482.23	3.69	0.04	10.64	5.73	**89.36**	0.04	0.42	0.68
911.64	10.89	0.07	27.30	2.98	0.04	**91.35**	0.24	0.39
960.79	17.52	15.10	0.18	5.19	4.15	11.09	8.30	29.34
979.89	0.24	14.59	0.07	4.42	0.17	0.05	**95.83**	10.77

TABLE 3: MAC (%) comparison for the prototype model(Mesh C_a)

7 RESULTS: SPRING JOINT UPDATING

The C_a prototype *FE* model discussed in Section 5 was modified by adding spring joints to both of the H-frames welded connections. The spring joint configuration shown in Figure 1 was adopted. The initial spring stiffness values were chosen based on the surrounding horizontal frame elements. By doubling the axial (EA/L), transverse $(12EI/L^3)$ and rotational $(4EI/L)$ stiffness terms, the following values were used as starting spring estimates $\{k_{x0},\ k_{z0},\ k_{\theta 0}\} = \{3.30 \times 10^9,\ 4.48 \times 10^9,\ 3.02 \times 10^6\}$ [N/m, N/m, N.m/rad].

Before attempting to update the local spring parameters, a global update of the H-frame spring model was performed. Two design parameters common to all frame elements were selected, EI and ρA, with the first 5 experimental modes being used to drive the update. The results of the global update are summarised in Table 4(c) and are similar to those obtained from the global update of the C_a prototype model. The normalised frequency errors $\bar{\omega}$ shown in Table 4(c) reveal that although the errors for modes 2 and 5 have been reduced, the errors for the remaining modes have increased. The design parameter perturbations shown in Table 4(c) also reveal that the updating process caused a 12% increase in the H-frame's mass, a result that is not consistent with the true mass of the structure.

A second update of the spring joint H-frame model was attempted, this time using the 3 springs at the welded connections as design parameters. A single global stiffness term EI was also included in the update, giving 4 design parameters being driven by 5 measured modes - it was assumed that the stiffness parameters at the 2 welded connections were identical. The results of the spring joint update are summarised in Table 4(d). Comparing the natural frequency errors $\bar{\omega}$ before and after the update shows a significant improvement over the results obtained from the original global update. The perturbations to the design parameters presented in Table 4(d) indicate that the rotational spring stiffness k_θ was the most sensitive design parameter during the update. This result is consistent with those obtained from the local update of the C_a prototype model.

8 RESULTS: GEOMETRIC OFFSET UPDATING

The representation of the welded joints was also approached using the geometric offset method. Each joint was represented by three partly rigid frame elements as shown by Figure 2. The 2 joints were again treated as being identical where it was assumed that the upper and lower vertical offsets were the same(say a_V), and that the 2 horizontal offsets (say a_H) were the same. Initial values for the offset parameters were specified as $a_H = 20$ [mm], and $a_V = 3.12 \times 10^{-6}$ [mm]. Using the first 5 modes to again drive the updating process the results of updating the partly rigid frame elements are summarised in Table 4(e). An inspection of the natural frequency errors in Table 4(e) reveals the success of the updating exercise. The updated model now predicts the measurement set with a maximum error of 0.85%. Viewing the perturbations to the offset parameters listed in Table 4(e), shows however that the horizontal offset a_H has been forced to become negative.

The nature of the geometric offset approach is to stiffen the region surrounding the joint by using rigid connections(a geometric offset). If the stiffness of the jointed region has to be reduced however, the length of the offset must be decreased, and in this case has been forced to become negative. While a negative offset can be visualized by extending the length of a beam beyond the neutral axes of the adjoining beams, it is probably more appropriate to consider the offset dimension as simply another means of parameterising the joint. By considering the local stiffness matrix for the partly rigid beam element, equation (5), it can also be seen that the offset parameter preserves to a certain extent the relative magnitudes of the stiffness terms -ie we still have a rough L, L^2, L^3 relationship between terms.

9 CONCLUSIONS

Three different methods for parameterising welded joints in a simple H-frame structure were discussed, and the results of updating an *FE* model using beam elements presented. In all cases it was found that for the first five bending modes, two modes in particular(modes 2 and 5), were extremely sensitive to the stiffness representation of the joint. By parameterising the jointed region and updating the H-frame model, the natural frequency errors for the first five bending modes were

reduced.

A common problem for all of the H-frame updating exercises was explaining why modes 2 and 5 were so poorly estimated when using a beam element representation of the joints. The answer to this, may simply be that the localised deformation of the joint requires a more detailed element representation - plate elements for example. If this is indeed the case, the problem of adequately modelling welded joints may first require the *FE* reduction of a detailed joint model. The reduced joint model may then be connected to surrounding substructures which for example consist of beam elements

APPENDIX: DERIVATION OF EIGEN SENSITIVITY UP-DATE EQUATION

The finite element updating of a system described by the familiar second order equation $M\ddot{x} + Kx = 0$, and the corresponding eigenvalue equation $K\phi = \lambda M\phi$, can be achieved by first linearising the analytical eigenvalue λ using a set of specified design parameters $\theta \in R^d$. This expansion/linearisation process is shown by equation (7), where θ_o represents the current state of the design parameters. With the analytical eigenvalue linearised, a residual ε between the measured λ_m and analytical λ eigenvalues, can be expressed as shown by equation (9).

$$\lambda(\theta) = \lambda(\theta_o) + \left.\frac{\partial\lambda}{\partial\theta}\right|_{\theta=\theta_o}(\theta-\theta_o) \quad (7)$$

$$\lambda(\theta) = \lambda_o + \frac{\partial\lambda}{\partial\theta_o}\delta\theta \quad (8)$$

$$\varepsilon \equiv \lambda_m - \lambda(\theta) = (\lambda_m - \lambda_o) - \frac{\partial\lambda}{\partial\theta_o}\delta\theta = \delta z - S_o\delta\theta \quad (9)$$

The objective of the updating exercise is to then minimize the norm of the residual vector ε ($\equiv \lambda_m - \lambda = \delta z - S_o\delta\theta$). This minimization process can be achieved by defining an appropriate scalar cost function J, and minimizing J with respect to the design parameter perturbation vector $\delta\theta$. A common cost function is to include weighted norms of both the eigenvalue residual ε, and design parameter perturbation $\delta\theta$, as shown by equation (10). By choosing symmetrical weighting matrices $W_{\varepsilon\varepsilon}$ and $W_{\theta\theta}$, the cost function can be simplified to equation (11).

$$J = \varepsilon^T W_{\varepsilon\varepsilon} \varepsilon + \alpha \delta\theta^T W_{\theta\theta} \delta\theta \quad (10)$$

$$J = \delta z^T W_{\varepsilon\varepsilon}\delta z - 2\delta z^T W_{\varepsilon\varepsilon}S_o\delta\theta + \delta\theta^T(S_o^T W_{\varepsilon\varepsilon}S_o + \alpha W_{\theta\theta})\delta\theta \quad (11)$$

The cost function defined by (11) is simply a scalar function of the scalar variables $\delta\theta_1, \delta\theta_2, ...\delta\theta_d$, and can be minimized in the usual fashion, ie: $\partial J/\partial\delta\theta_1 = ...\partial J/\partial\delta\theta_d = 0$. A vector equivalent of the d equations, $\partial J/\partial\delta\theta_i$ is expressed by equation (12). Simplifying (12) results in the design parameter perturbation vector $\delta\theta$ given by (14).

$$\frac{\partial J}{\partial\delta\theta} = 0 = -2(\delta z^T W_{\varepsilon\varepsilon}S_o)^T + (D + D^T)\delta\theta \quad (12)$$

$$0 = -2S_o^T W_{\varepsilon\varepsilon}\delta z + 2(S_o^T W_{\varepsilon\varepsilon}S_o + \alpha W_{\theta\theta})\delta\theta \quad (13)$$

$$\delta\theta = [S^T W_{\varepsilon\varepsilon}S_o + \alpha W_{\theta\theta}]^{-1}S_o^T W_{\varepsilon\varepsilon}\delta z \quad (14)$$

REFERENCES

[1] **Lindholm, B.**, *A Bayesian Statistics Approach to Updating Finite Element Models with Frequency Response Data(Part II: Application)*, Proceedings of the 14th International Modal Analysis Conference, pp. 1458–1464, 1996.

[2] **Alvin, K.**, *Finite Element Model Update via Bayesian Estimation and Minimization of Dynamic Residuals*, AIAA Journal, Vol. 35, No. 5, pp. 879–886, 1997.

[3] **Mottershead, J., Friswell, M., Ng, G. and Brandon, J.**, *Experience in Mechanical Joint Model Updating*, 19th International Seminar on Modal Analysis, pp. 481–495, 1994.

[4] **Friswell, M. and Mottershead, J.**, Finite Element Model Updating in Structural Dynamics, Kluwer Academic Publishers, 1995.

[5] **Fox, R. and Kapoor, M.**, *Rates of Change of Eigenvalues and Eigenvectors*, AIAA Journal, Vol. 6, No. 12, pp. 2426–2429, 1968.

[6] **Link, M.**, *Updating of Analytical Models - Basic Procedures and Extensions*, NATO Advanced Study Institute: Modal Analysis and Testing, pp. 335–355, 1998.

[7] **Collins, J., Hart, G., T.K., H. and Kennedy, B.**, *Statistical Identification of Structures*, AIAA Journal, Vol. 12, No. 2, pp. 185–190, 1974.

[8] **Blakely, K. and Walton, W.**, *Selection of Measurement and Parameter Uncertainties for Finite Element Model Revision*, Proceedings of the 2nd International Modal Analysis Conference, pp. 82–88, 1984.

[9] **Ahmadian, H., Mottershead, J. and Friswell, M.**, *Joint Modelling for Finite Element Model Updating*, Proceedings of the 14th International Modal Analysis Conference, pp. 591–596, 1996.

[10] **Brown, D., Allemang, R. and Zimmerman, R.**, *Parameter Estimation Techniques for Modal Analysis*, Society of Automotive Engineers, pp. 1–19, 1979.

[11] **Levy, E.**, *Complex-Curve Fitting*, IRE Transactions on Automatic Control, Vol. 4, pp. 37–43, 1959.

[12] **Matlab5**, Signal Processing Toolbox (Ver 4.0.1) Users Guide, MathWorks Inc, 1996.

[13] **Balmes, E.**, Structural Dynamics Toolbox, Users Guide Version 3, Scientific Software Group, 1997.

[14] **O'Callahan, J. and Li, P.**, *Serep Expansion*, Proceedings of the 14th International Modal Analysis Conference, pp. 1258–1264, 1996.

Mode ID	Experimental ω[Hz]	Initial FEM ω[Hz], (ϖ[%])	Updated FEM ω[Hz], (ϖ[%])
1	77.13	78.51, (1.79)	74.26, (-3.72)
2	137.60	147.31, (7.06)	139.33, (1.26)
3	300.90	298.90, (-0.66)	282.84, (-6.00)
4	404.98	408.03, (0.75)	385.96, (-4.70)
5	482.23	523.31, (8.52)	495.16, (2.68)

Design parameter θ	Initial value θ_0	Updated value θ_{up}	θ_{up}/θ_0
EI [Pa.m^4]	17015	15223	0.895

(a) Global parameter update of C_a prototype model

Mode ID	Experimental ω[Hz]	Initial FEM ω[Hz], (ϖ[%])	Updated FEM ω[Hz], (ϖ[%])
1	77.13	78.51, (1.79)	75.17, (-2.54)
2	137.60	147.31, (7.06)	134.91, (-1.95)
3	300.90	298.90, (-0.66)	301.1, (0.07)
4	404.98	408.03, (0.75)	404.47, (-0.13)
5	482.23	523.31, (8.52)	482.42, (0.04)

Design parameter θ	Initial value θ_0	Updated value θ_{up}	θ_{up}/θ_0
EI_X [Pa.m^4]	17015	8385	0.493
EI_Z [Pa.m^4]	17015	18400	1.081

(b) Local parameter update of C_a prototype model

Mode ID	Experimental ω[Hz]	Initial FEM ω[Hz], (ϖ[%])	Updated FEM ω[Hz], (ϖ[%])
1	77.13	79.31, (-2.83)	72.67, (-5.78)
2	137.60	151.45, (10.07)	139.82, (1.61)
3	300.90	299.05, (-0.61)	273.31, (-9.17)
4	404.98	411.55, (-1.62)	376.71, (-6.98)
5	482.23	539.36, (11.85)	500.00, (3.68)

Design parameter θ	Initial value θ_0	Updated value θ_{up}	θ_{up}/θ_0
EI [Pa.m^4]	17015	15826	0.930
ρA [kg/m]	2.814	3.159	1.123

(c) Global parameter update of spring joint model

Mode ID	Experimental ω[Hz]	Initial FEM ω[Hz], (ϖ[%])	Updated FEM ω[Hz], (ϖ[%])
1	77.13	79.31, (2.83)	75.16, (-2.55)
2	137.60	151.45, (10.07)	135.41, (-1.59)
3	300.90	299.05, (-0.61)	298.82, (-0.69)
4	404.98	411.55, (-1.62)	402.89, (-0.52)
5	482.23	539.36, (11.85)	482.51, (0.06)

Design parameter θ	Initial value θ_0	Updated value θ_{up}	θ_{up}/θ_0
k_x [N/m]	3.30×10^9	3.24×10^9	0.981
k_z [N/m]	4.48×10^9	4.35×10^9	0.971
$k_{\theta y}$ [N.m]	3.02×10^6	273725	0.091
EI [Pa.m^4]	17015	17015	1.000

(d) Local and global parameter update of spring joint model

Mode ID	Experimental ω[Hz]	Initial FEM ω[Hz], (ϖ[%])	Updated FEM ω[Hz], (ϖ[%])
1	77.13	80.08, (3.82)	76.70, (-0.56)
2	137.60	154.83, (12.52)	138.77, (0.85)
3	300.90	299.28, (-0.54)	299.18, (-0.57)
4	404.98	413.67, (2.15)	405.73, (0.19)
5	482.23	553.71, (14.82)	482.17, (-0.01)

Design parameter θ	Initial value θ_0	Updated value θ_{up}	θ_{up}/θ_0
a_H [m]	0.02	-0.0283	-1.415
a_V [m]	3.12×10^{-6}	3.12×10^{-6}	1.000
EI [Pa.m^4]	17015	17132	1.007

(e) Local and global parameter update of geometric offset joint model

TABLE 4: H-frame FE model updating results